JOURNAL OF GEOPHYSICAL RESEARCH, VOL. 106, NO. D15, PAGES 17,253–17,266, AUGUST 16, 2001

Prevalence of ice-supersaturated regions in the upper troposphere: Implications for optically thin ice cloud formation

Eric J Jensen,[1] Owen B Toon,[2] Stephanie A. Vay,[3] Joëlle Ovarlez,[4] Randy May,[5,6] T. P Bui,[1] Cynthia. H. Twohy,[7,8] Bruce W. Gandrud,[7] Rudolf F. Pueschel,[1] and Ulrich Schumann[9]

Abstract. In situ measurements of water vapor and temperature from recent aircraft campaigns have provided evidence that the upper troposphere is frequently supersaturated with respect to ice. The peak relative humidities with respect to ice (RHI) occasionally approached water saturation at temperatures ranging from -40°C to -70°C in each of the campaigns. The occurrence frequency of ice supersaturation ranged from about 20% to 45% Even on flight segments when no ice crystals were detected, ice supersaturation was measured about 5–20% of the time. A numerical cloud model is used to simulate the formation of optically thin, low ice number density cirrus clouds in these supersaturated regions. The potential for scavenging of ice nuclei (IN) by these clouds is evaluated. The simulations suggest that if less than about 5 x 10^{-3} to 2 x 10^{-2} cm^{-3} ice nuclei are present when these supersaturations are generated, then the cirrus formed should be subvisible. These low ice number density clouds scavenge the IN from the supersaturated layer, but the crystals sediment out too rapidly to prevent buildup of high supersaturations If higher numbers of ice nuclei are present, then the clouds that form are visible and deposition growth of the ice crystals reduces the RHI down to near 100%. Even if no ice clouds form, increasing the RHI from 100% to 150% between 10 and 10.5 km results in a decrease in outgoing longwave radiative flux at the top of the atmosphere of about 8 W m^{-2}. If 0.02–0.1 cm^{-3} IN are present, the resulting cloud radiative forcing reduces the net radiative flux several watts per square meter further. Given the high frequency of supersaturated regions without optically thick clouds in the upper troposphere, there is a potential for a climatically important class of optically thin cirrus with relatively low ice crystal number densities. The optical properties of these clouds will depend very strongly on the abundance of ice nuclei in the upper troposphere.

[1]NASA Ames Research Center, Moffett Field, California
[2]Laboratory for Atmospheric and Space Physics, Department of Atmospheric and Oceanic Science, University of Colorado, Boulder, Colorado
[3]NASA Langley Research Center, Hampton, Virginia
[4]Laboratoire de Meteorologie Dynamique, Ecole Polytechnique, Palaiseau, France
[5]Jet Propulsion Laboratory, Pasadena, California
[6]Now at SpectraSensors, Inc , Altadena, California
[7]National Center for Atmospheric Research, Boulder, Colorado
[8]Now at Oregon State University, Corvallis, Oregon
[9]Deutsches Zentrum für Luft- und Raumfahrt, Institut für Physik der Atmosphäre, Oberpfaffenhofen, Germany

Paper number 2000JD900526
0148-0227/01/2000JD900526$09 00

1. Introduction

In the lower troposphere at temperatures above 0°C, relative humidities with respect to liquid water never exceed saturation by more than a few percent [*Pruppacher and Klett*, 1997]. However, recent upper tropospheric in situ observations have shown that large supersaturations with respect to ice can exist at low temperatures [*Heymsfield et al.*, 1998; *Gierens et al.*, 1999; *Jensen et al.*, 1998]. Also, laboratory experiments have shown that large ice supersaturations are required to freeze sulfate aerosols [*Koop et al.*, 1998] and trigger cloud formation. The occurrence of ice supersaturation in the upper troposphere has a few important implications. First, the maximum observed humidities in cloud-free air provide an indication of the threshold for ice nucleation and cirrus formation [*Heymsfield et al*, 1998; *Jensen et al.*, 1998]. Second, if a small number

of ice nuclei (IN) are available, then optically thin cirrus could form in these supersaturated regions These optically thin clouds may scavenge the IN from the upper troposphere Finally, water vapor is an important greenhouse gas, particularly in the cold upper troposphere The common occurrence of ice supersaturation in the upper troposphere may imply higher water vapor concentrations than previously thought

In this study, we combine data from several field experiments to examine the frequency of supersaturation in the upper troposphere. Cloud sampling instrumentation included in these missions is used to separate cloudy and clear regions The potential for formation of ice clouds with crystal number densities too low for detection by the available instrumentation is evaluated with model simulations The model calculations are used to investigate the cloud sensitivity to IN number density and to evaluate the potential impact of the clouds on the radiation budget.

2. In Situ Upper Tropospheric Humidity Measurements

Information about humidity in the upper troposphere has been extremely scarce primarily because the standard humidity sensors used on radiosondes are unreliable at temperatures below about -40°C. Comparisons between Väisälä sonde and cryogenic hygrometer humidity measurements at low temperatures have shown that the Väisäla sonde substantially underestimates the humidity [*Miloshevich and Heymsfield*, 1998] Hence, our accurate information about upper tropospheric humidity on small spatial scales is primarily limited to focused measurement campaigns using sophisticated in situ water vapor instruments on either aircraft or balloons. The Measurement of Ozone and Water Vapor by Airbus In-Service Aircraft (MOZAIC) program, using carefully calibrated humidity sensors on commercial aircraft, has also provided useful upper tropospheric humidity data [*Gierens et al* , 1999].

For this study, we use data from four aircraft campaigns: The 1996 Subsonic Aircraft: Contrail and Cloud Effects Special Study (SUCCESS) experiment was conducted over the central and western United States; the 1997 Subsonic Assessment Program (SASS) Ozone and Nitrogen Oxides Experiment (SONEX) provided sampling over the North Atlantic; the 1997 Pollution from Aircraft Emissions in the North Atlantic Flight Corridor (POLINAT 2) experiment was also based in the North Atlantic; and the 1998 Convection and Moisture Experiment (CAMEX) experiment primarily consisted of flights in the vicinity of Florida. The spatial distribution of upper tropospheric (T <-40°C) sampling from these missions is shown in Plate 1

During the SUCCESS and SONEX experiments, the water vapor mixing ratio was measured with a near-IR tunable Diode Laser Hygrometer (DLH) mounted on the NASA DC-8 [*Vay et al* , 1998, 2000]. This external path instrument provides accurate water vapor measurements both in cloud-free conditions and within clouds Temperature and pressure were measured with the Meteorological Measurement System (MMS) on board the DC-8. During SONEX a pressure leak was present in the MMS system, resulting in a high bias of about 1 K in the temperature measurement [P. Bui, personal communication, 1999] Also, a small amount of water vapor was present in the DLH internal optical path during SONEX, resulting in a measurement offset of about +10 ppmv [*Vay et al.*, 2000] This offset substantially affects the relative humidities only at the lowest temperatures sampled (+10 ppmv at 200 mbar corresponds to a relative humidity with respect to ice (RHI) offset of 20% at -60°C; at -40°C the RHI offset is only about 2%). We have subtracted 10 ppmv from the reported SONEX DLH values and used MMS temperatures corrected for the pressure leak (The corrected MMS temperatures are now available on the SONEX data archive.) The DLH offset probably decreased with decreasing temperature; so we may be underestimating humidities at the lowest temperatures Given uncertainties of 10% for water vapor mixing ratio and 0.5 K for temperature, the resulting uncertainty in RHI is about 15% for SUCCESS. The RHI uncertainty from the SONEX experiment must be somewhat larger due to the MMS pressure leak and water vapor within the DLH optics, but how much larger is not possible to quantify.

Water vapor mixing ratios from the POLINAT 2 experiment were measured with a cryogenic frost point hygrometer along with an air pressure sensor, on board the Deutsches Zentrum für Luft und Raumfahrt (DLR) Falcon aircraft [*Ovarlez et al.*, 2000; *Schumann et al* , 2000]. The relative humidities are then deduced by using the static air pressure and air temperature measurements from the Falcon aircraft equipment [*Quante et al* , 1996]. The RHI uncertainty is about 10%, resulting from an uncertainty of 4% in water vapor mixing ratio and 0 5 K in the static temperature. Intercomparison between the SONEX DLH (corrected as described above) and POLINAT 2 cryogenic hygrometer water vapor measurements from coordinated flights showed agreement to within the measurement uncertainties, although the DLH water vapor mixing ratios were systematically about 10% higher than the cryogenic values [*Vay et al* , 2000]

During the CAMEX experiment, water vapor was measured with the Jet Propulsion Laboratory (JPL) laser hygrometer [*Hintsa et al* , 1999] on board the DC-8 The MMS system was also included on the DC-8 during this mission. Since CAMEX was focused on sampling of tropical hurricanes, some of the flight time was spent in regions with large ice water contents and/or very strong vertical motions. For this study, we use the MMS vertical wind speed measurements to exclude the time periods within violent convective regions.

Instrumentation for sampling cloud properties was also included in most of these missions. During SUCCESS, several cloud instruments were included on the DC-8 The most useful of them for determining cloud properties throughout the mission without excessive analysis labor is the Counterflow Virtual Impactor (CVI) [*Twohy et al.*, 1997]. This instrument provides ice water content and ice number density at 1 Hz. Only particles larger than about 5 μm diameter were sampled by the CVI, and ice crystal number concentrations less than 0 1 cm-3 were not reported due to noise at low altitudes. During SONEX and CAMEX, the DC-8 included a Forward-Scattering Spectrometer Probe (FSSP-300) [*Baumgardner et al* , 1992]. The FSSP-300 provides information about particle size distribution at diameters ranging from 1 - 40 μm. This instrument should be useful for distinguishing clear and cloudy regions The FSSP ice number density threshold (due to sample volume limitations) is similar to the CVI (0.1 cm^{-3}).

The flight planning strategies for the three missions were very different. During SUCCESS, an effort was made to sample regions where the relative humidity was forecast to be high such that cirrus and/or persistent contrails would be likely. In SONEX, part of the time, the flight planning attempted to avoid clouds or high humidity regions, and much of the time the issue of clouds was ignored. Hence, we might have expected to generally see higher relative humidities during SUCCESS than during SONEX or POLINAT. As is shown in Plate 2, the RHIs during SONEX and POLINAT were just as high as those during SUCCESS; so it appears that meteorological variations played a larger role than flight planning strategies. During CAMEX, considerable amounts of time were spent in or near hurricanes; hence, we anticipated that a large fraction of the data would show high relative humidities.

Plate 2 shows frequency distributions of RHI and temperature from the four field experiments This figure includes both cloudy and cloud-free sampling periods Time periods for which the MMS instrument indicated vertical wind speeds larger than 1 m s^{-1} are excluded. This restriction substantially affects only the CAMEX RHI frequency distributions During CAMEX, regions with very large updrafts in the vicinity of hurricanes were sampled. Within these strong updrafts, humidities were well in excess of water saturation. Even with the $w < 1$ m s^{-1} restriction water saturation was detected on several occasions during CAMEX, but these occurrences were typically the edges of strong updrafts. The frequencies of ice supersaturation for different missions are given in Table 1.

The RHI statistics from the four missions generally indicate a consistent result: At temperatures below -40°C, substantial supersaturations with respect to ice are common, with RHI values sometimes approaching water saturation. This result is consistent with previous analyses of upper tropospheric relative humidities using different instrumentation [*Heymsfield et al* , 1998; *Gierens et al* , 1999]. Using the MOZAIC data set, *Gierens et al.* [1999] reported ice supersaturation at the flight level of commercial air traffic about 13 5% of the time. Hence, the common occurrence of upper tropospheric ice supersaturations has now been observed in several geographic regions with several different water vapor instruments.

Table 1. Fraction of Observations with RHI > 100% (in percent)

	All data[a]	Clear[b]	Cloudy[c]
SUCCESS	21 4	10 2	49 3
SONEX	22 9	20 7	88 6
POLINAT 2	42 6		
CAMEX	45 0	9 6	86 7

[a]Both cloudy and cloud-free time periods are included Time periods with vertical wind speeds larger than 1 m s^{-1} or temperatures greater than -40°C are excluded

[b]CVI number density of <0 1 cm^{-3} for SUCCESS; FSSP volume of <40 $\mu m^3/cm^{-3}$ for SONEX and CAMEX

[c]CVI number density of ≥0 1 cm^{-3} for SUCCESS; FSSP volume of ≥40 $\mu m^3/cm^{-3}$ for SONEX and CAMEX

Another notable feature in the frequency distributions is a lack of observed low humidities at low temperatures. Particularly in the SONEX and POLINAT 2 missions there appears to be a well-defined RHI lower limit that increases with decreasing temperature. One possible explanation for this feature is that as air parcels rise and cool in the troposphere, their relative humidity increases. Even a relatively dry (RHI = 10%) air parcel at -40°C will be supersaturated if it is cooled adiabatically to -65°C. Hence, at the lowest temperatures in the upper troposphere, relative humidities should generally be high There are two possibilities for generating extremely dry air in the extreme upper troposphere at midlatitudes: Intrusions of stratospheric air with water vapor mixing ratios as low as 4-5 ppmv can result in RHIs less than 10% at -60°C and 200 mbar. A potential dehydration mechanism is baroclinic disturbances that advect air parcels upward and poleward (along sloping isentropic surfaces), followed by freeze drying of the air by cirrus clouds at temperatures below typical midlatitude tropopause temperatures [*Kelly et al* , 1991] The flow then returns the dry air to lower latitudes. Apparently, neither of these mechanisms for generating low RHIs substantially affected the regions sampled in these missions.

Plate 3 shows the RHI frequency distributions during the times when cloud microphysical sampling instruments indicated that no clouds were present. For the SUCCESS data set we use the CVI number de3-sity threshold of 0 1 cm^{-3} as an indicator of clouds. For SONEX and CAMEX, an FSSP volume of 40 μm^3-

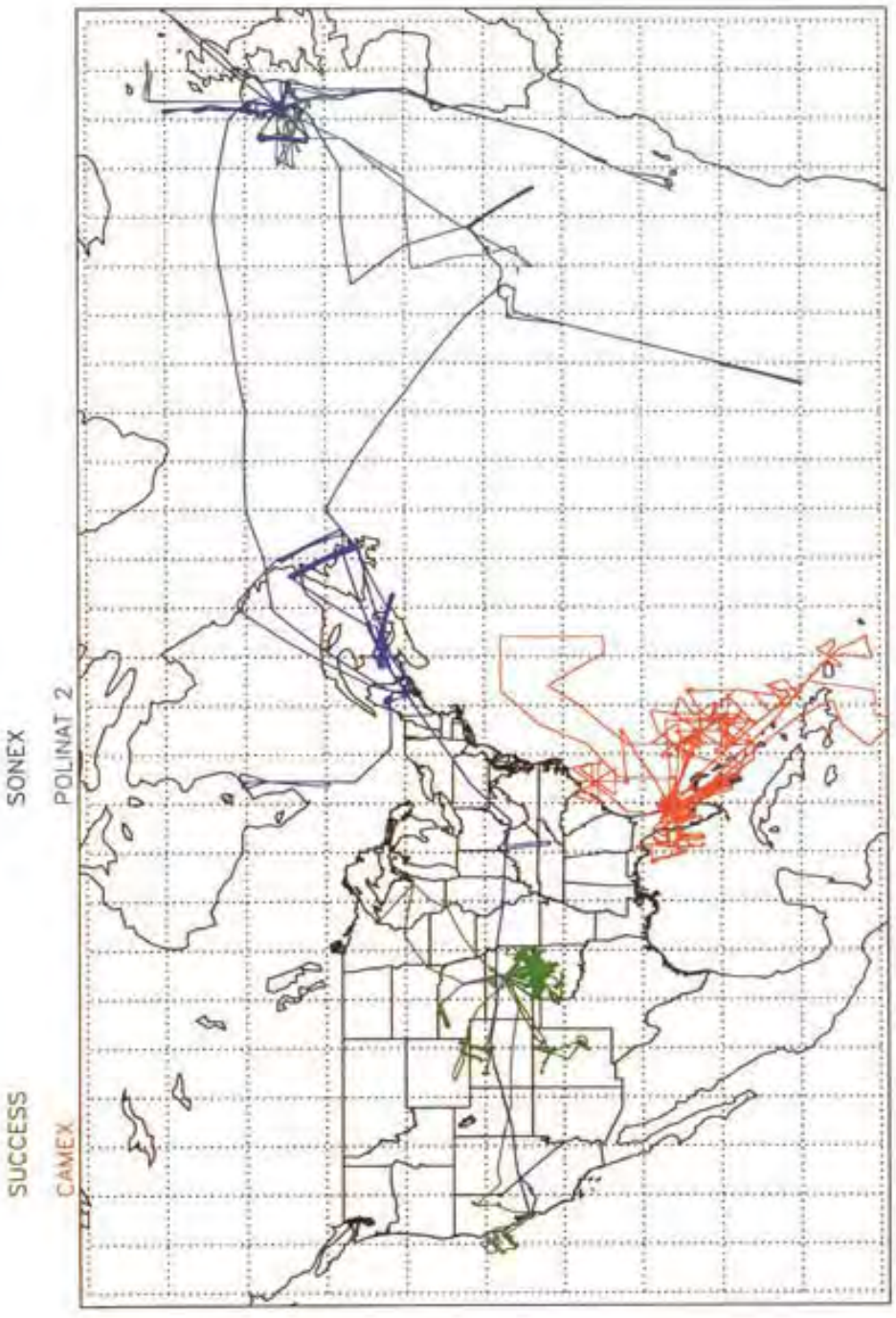

Plate 1. Flight paths from SUCCESS (April 15 to May 15, 1996), SONEX (October 7 to November 12, 1997), POLINAT 2 (September 19 to October 23, 1997), and CAMEX (August 13 to September 22, 1998) are shown. Only time-periods during which the temperature was below –40°C are included.

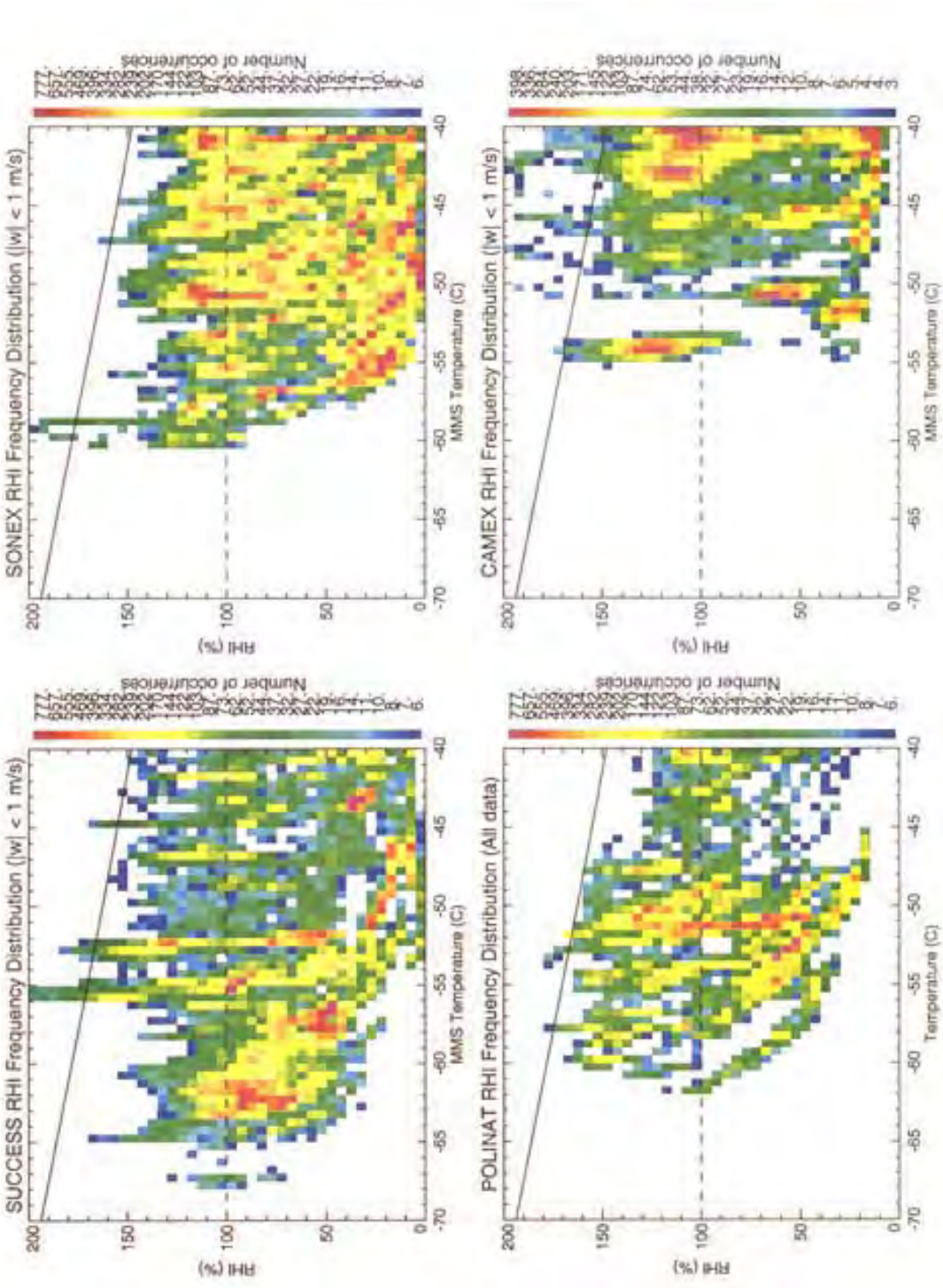

Plate 2. Probability distribution of 1-s observations plotted versus temperature and RHI. The temperature and RHI bin sizes were 0.5 K and 5%, respectively. All data (clear and cloudy) are included. The dashed line shows saturation with respect to ice, and the solid line corresponds to saturation with respect to liquid water.

cm^{-3} is used This volume density is equivalent to a cloud with 0.1 cm^{-3} 10-μm diameter ice crystals Although the frequency of supersaturation in the cloud-free sampling times is lower than that for the entire data set (see Table 1), it is still relatively high.

Table 1 also shows the frequency of supersaturation within regions where ice crystals were detected. As expected, these frequencies are very high, and the humidities are not limited to values just above ice saturation (see the discussion in section 3). Large supersaturations (RHIs up to 150%) can exist within cloudy regions.

An important caveat here is that the RHI statistics from these missions do not necessarily represent typical climatological upper tropospheric humidity statistics. They are limited data sets with measurements only at a limited range of times and locations The SUCCESS and CAMEX data sets were no doubt biased, since flight planning was focused on sampling cloudy regions. During SONEX and POLINAT 2, no apparent effort was made to seek clouds; however, *Ovarlez et al.* [2000] noted that the humidities measured during POLINAT 2 were in general much higher than those encountered during earlier POLINAT missions. Hence, although these data sets suggest that a substantial fraction of the upper troposphere is supersaturated with respect to ice, the numbers in Table 1 should not be taken as climatological means.

3. Limitation of Supersaturation by Clouds

If no cloud formation were to occur, an air parcel with an initial RHI of 30% would reach an RHI of >200% as it ascends adiabatically through the upper troposphere (7–10 km) As soon as cloud formation is initiated by ice nucleation, the continued increase in RHI is prevented by depletion of the vapor due to ice crystal deposition growth. Measurements of maximum relative humidities have been used to estimate the threshold for ice nucleation in the upper troposphere [*Heymsfield et al.*, 1998; *Jensen et al* , 1998].

The ability of ice crystals to halt the humidity increase in a cooling parcel depends upon the cooling rate and the number of ice crystals nucleated If very few ice crystals nucleate, then the RHI may continue to rise above the threshold value for ice nucleation (RHI_{nuc}) i.e , the deposition growth of the small number of ice crystals may be insufficient to stop the continued increase of RHI due to cooling. We have run a series of parcel model simulations to see how far the RHI can exceed RHI_{nuc}. For these experiments we use our detailed ice microphysics model with just sulfate aerosols and ice crystals. The sulfate aerosol freezing expressions given by *Tabazadeh et al.* [2000] are used. This parameterization is designed to match laboratory measurements of sulfuric acid solution aerosol freezing [*Koop et al.*, 1998]. The resulting code predicts thresholds for ice nucleation on the sulfate aerosols ranging from about 160 to 170%, depending on the temperature. We begin the simulations with a temperature of -55°C, an RHI of 110%, and no ice crystals present. As the parcel cools, a fraction of the aerosols freeze resulting in ice crystals that deplete the vapor by deposition growth. The simulations are run until the RHI reaches its maximum value and begins to decrease. The parcels rise about 500 m and cool about 4–5 K before nucleation occurs.

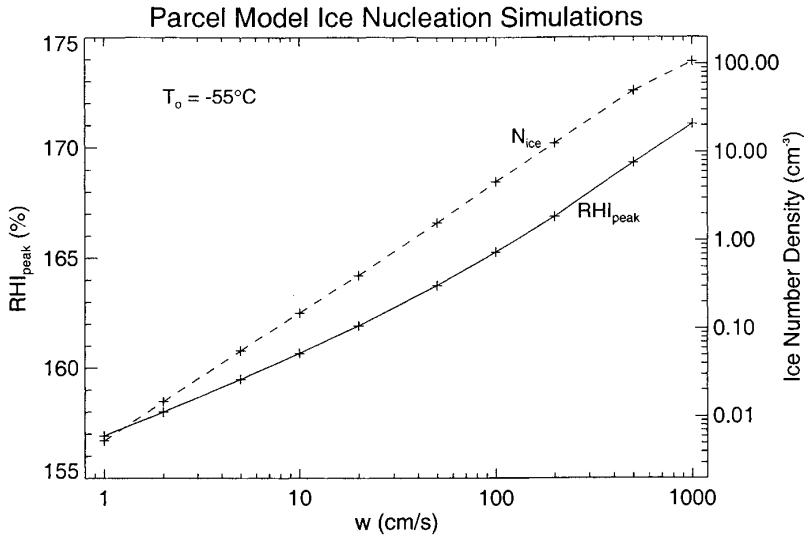

Figure 1. Peak relative humidity with respect to ice and peak ice crystal number density plotted versus updraft speed from a series of parcel model simulations. These calculations show that in moderately strong updrafts ($w \simeq$ 1–3 m s^{-1}), the RHI can rise several percent higher than the threshold for ice nucleation

Figure 1 shows the variation of peak ice number density and peak RHI with the updraft speed. As was described by *Jensen and Toon* [1994], the ice number density increases rapidly with cooling rate due to competition between growth of existing crystals and nucleation of new crystals. For updraft speeds of less than a few centimeters per second, the peak RHI is no more than a few percent larger than RHI_{nuc}. However, in strong updrafts ($w > 1$ m s^{-1}) the RHI may rise about 10% above RHI_{nuc} (from 160 to 170%). Hence, even if a large number of aerosols are available for ice nucleation, supersaturations substantially beyond the threshold value may occur in strong updrafts. As the ice crystals continue to grow, the RHI will drop below these peak values.

If an ice cloud exists in rising air, an equilibrium can develop in which the increase in supersaturation due to cooling balances the water vapor taken up by crystal deposition growth. *Khvorostyanov and Sassen* [1998] showed that equilibrium ice supersaturations of 1–10% can be maintained in clouds with typical cirrus ice number densities and vertical wind speeds of 1–20 cm s^{-1}. Further, they showed that cirrus should typically take about 0.5–2 hours before the RHI drops to its equilibrium value. During this relaxation time, the RHI will be somewhere between the equilibrium value and RHI_{nuc} (possibly briefly overshooting RHI_{nuc}). These calculations suggest that the substantial supersaturations observed within cirrus clouds are plausible

4. One-Dimensional Simulations of Cloud Formation in Supersaturated Regions

The instrumentation available during the aircraft missions described above was not optimized for sampling clouds with extremely low ice number densities In particular, the CVI lower detection threshold during SUCCESS was effectively 0 1 cm^{-3} due to noise under certain conditions.. Hence, it is possible that optically thin clouds with low ice number densities existed in many of the the supersaturated regions. *Rogers et al* [1998] reported ice nuclei measurements from an airborne diffusion chamber on board the DC-8 during SUCCESS More than 95% of their upper tropospheric measurements indicated IN number densities of less than 0 1 cm^{-3} active at temperatures greater than -40°C

To evaluate the potential for formation of cirrus in supersaturated regions, we use one-dimensional (1-D) simulations with a detailed cloud model. The model used is essentially identical to that described in several previous ice cloud formation studies [e.g , *Jensen et al* , 1998]. We use a simple version here, with only two particle types. ice nuclei and ice crystals. For each particle type, 30 radius bins are used spanning 0.2–5 μm for the IN and 0.5–250 μm for the ice crystals. IN number densities ranging from 1 x 10^{-3} to 0.5 cm^{-3} are used in the simulations. The physical processes simulated include ice nucleation, ice crystal growth and sublimation, crystal sedimentation, and vertical transport. A vertical grid spacing of 50 m is used We specify that ice nucleation occurs on these nuclei at a particular supersaturation with respect to ice. For the baseline simulation, we specify an IN number density of 0 02 cm^{-3} and a threshold RHI for nucleation of 133%. We use a single, size-independent threshold to control the number of ice crystals nucleated. In reality, the threshold would depend upon particle size and composition, so the number of ice crystals nucleated would vary with cooling rate and temperature. However, in this study, we are simply trying to examine the sensitivity of the cloud properties to the number of ice crystals nucleated. Also, we have avoided the complication of competition between heterogeneous and homogeneous ice nucleation by not allowing the RHI to reach the threshold for sulfate aerosol freezing. For a detailed analysis of potential upper tropospheric heterogeneous ice nucleation mechanisms, see *DeMott et al.* [1997].

We specify the initial vertical temperature profile based on the mid-latitude summertime U.S. Standard Atmosphere We assume there is a layer from 10 to 10 5 km (temperatures of -59° to -56°C) with RHI = 70%; above and below this layer, the RHI is set to 50% Vertical motion is specified throughout the model domain with a sinusoidal time variation For the baseline simulation, we use a period of 8 hours and an amplitude of 5 cm/s This imposed vertical motion results in a maximum vertical displacement of about 700 m. If no ice nucleation occurs, the RHI reaches a peak value of 150% (too small to initiate freezing of sulfuric acid aerosols)

Solar and infrared radiative fluxes are calculated in the model by using a two-stream radiative transfer code [*Toon et al.*, 1989]. The radiation code includes 44 bands (26 in the solar wavelength range (0.25–4.3 μm) and 18 at longer wavelengths (4.5–62.5 μm)). The water vapor continuum has been modified by following *Clough et al* [1992] Ice crystal single-scattering properties are calculated by using Mie scattering assuming equivalent volume spheres. The refractive index for ice is taken from *Warren* [1984] A fixed solar zenith angle of 60° is assumed. It is well known that the outgoing longwave radiation (OLR) at the top of the atmosphere is very sensitive to upper tropospheric water vapor concentrations [e.g., *Udelhoffen and Hartmann*, 1995]. In our 1-D simulation (without ice nucleation), the OLR decreases by 7.7 W m^{-2} as the RHI between 10 and 10.5 km increases from 100 to 150%. This increase is primarily driven by the decrease in temperature (the total amount of water vapor is not changed by the vertical motion) Hence, even if no ice clouds form, the existence of large ice supersaturations in the upper troposphere is very important for radiative budgets. Note that the impact of changes in relative humidity depe7.d very sensitively on the initial temperature profile used and the height at which the humidity is changed.

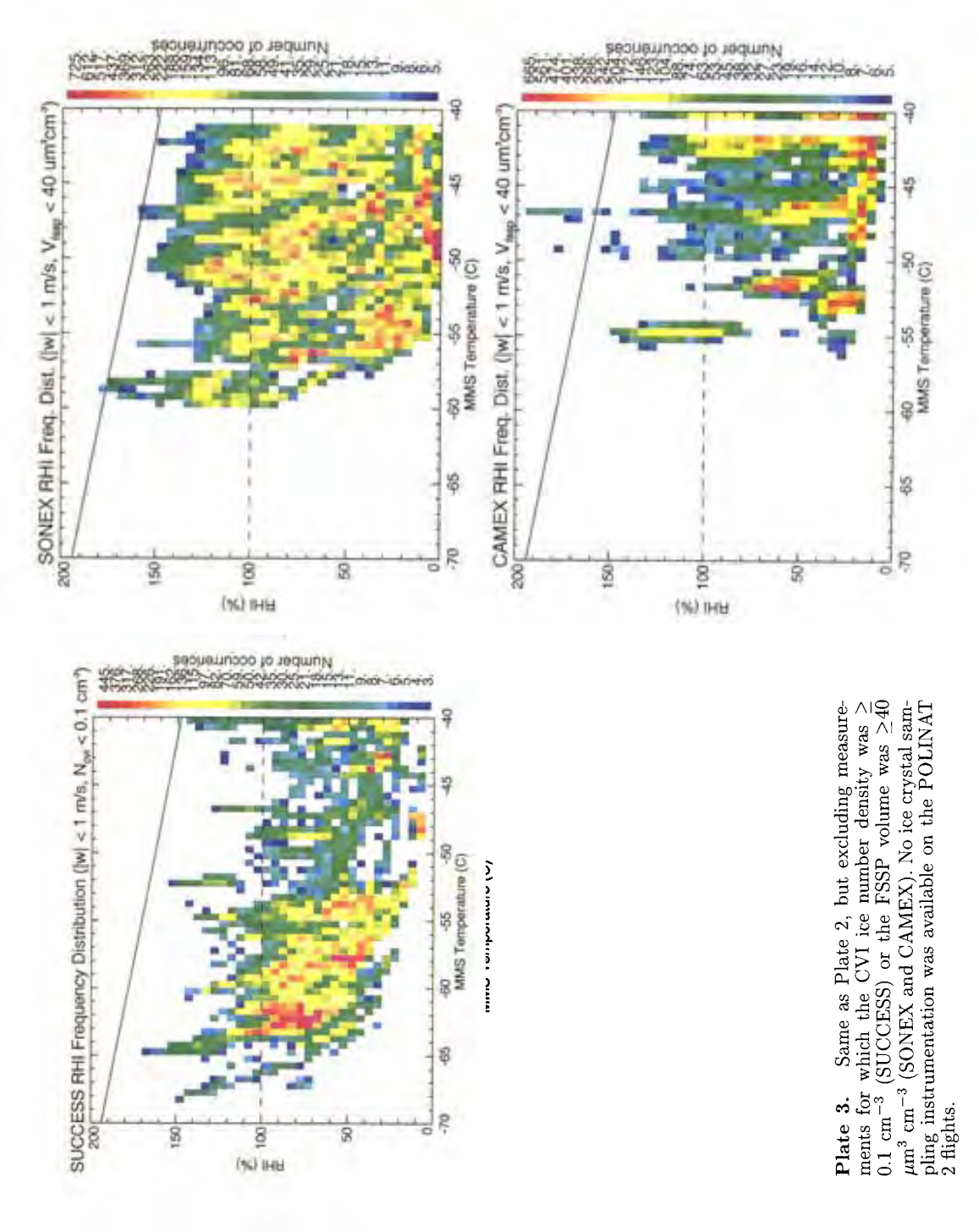

Plate 3. Same as Plate 2, but excluding measurements for which the CVI ice number density was ≥ 0.1 cm^{-3} (SUCCESS) or the FSSP volume was ≥ 40 μm^3 cm^{-3} (SONEX and CAMEX). No ice crystal sampling instrumentation was available on the POLINAT 2 flights.

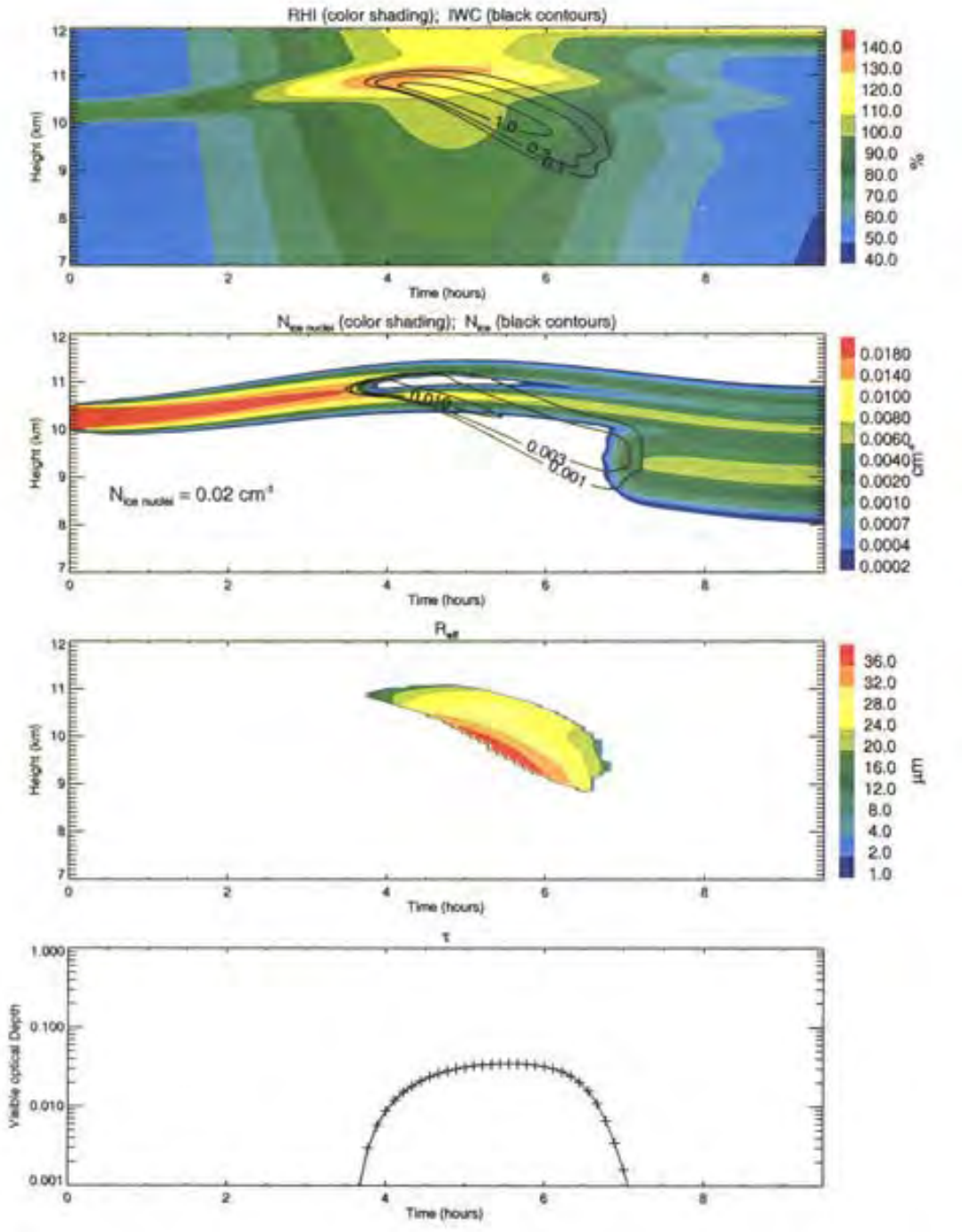

Plate 4. Results from the baseline simulation with an ice number density of 0.02 cm^{-3}. Panels (from top to bottom): relative humidity with respect to ice (color shading) and ice water content (milligrams per cubic meter, black contours) versus time and height; IN number density (color shading) and ice crystal number density (black contours, cm^{-3}); ice crystal effective radius; zenith visible cloud optical depth versus time.

The evolution of RHI, IN number density, and ice cloud properties in the baseline simulation are shown in Plate 4. Early in the simulation, the rising air cools and the humidity increases with time. When the RHI exceeds 133%, ice crystals rapidly nucleate until the IN are depleted. The ice crystals grow in the supersaturated environment, and the maximum crystal lengths reached are about 60 μm. The peak RHI reached in the simulation is 137%; hence, the ice crystal growth limited the peak RHI. Most of the ice sediments out of the original layer. The ice crystals do not penetrate more than about 1 km into the dry air below the supersaturated layer before they sublimate and release the IN. When the air descends (after 2 hours), the RHI is driven back down below 100%, and the remaining crystals sublimate. The net effect of the ice crystal formation and sedimentation is to clear out the IN from the layer and deposit them just below. The net reduction of RHI in the layer is about 8 3%

The zenith visible optical depth of the cloud is shown on the bottom panel of Plate 4. The peak optical depth reached in the baseline simulation is 0 035, which suggests that the cloud would just barely be visible to an observer on the ground Since we are controlling the ice crystal number density by specifying rapid nucleation of all available IN at a specific RHI, changing the threshold (assumed to be 133% here) does not dramatically change the cloud microphysical or optical properties. However, the clouds would be much more extensive if the nucleation threshold were lower.

We have run a large number of these simulations to test the sensitivities to the number density of IN available, the temperature at which the cloud forms, and the cooling rate. Results from these sensitivity tests are shown in Plate 5 At relatively low IN number densities (<5 x 10^{-3} to 2 x 10^{-2} cm^{-3}), only subvisible clouds form, and the ice crystals grow to lengths of 40–120 μm depending upon the duration of the supersaturation. Also, at low IN number densities in the 8-hour wave simulations, ice crystal sedimentation effectively clears the IN out of the supersaturated layer. The optical depth of the clouds increases rapidly with increasing IN number density. For the largest IN number densities observed during SUCCESS (>0.1 cm^{-3}), the clouds formed would be clearly visible from the ground. In the simulations with IN number densities larger than about 0 05 cm^{-3}, the ice crystals do not grow large enough to sediment out and scavenge the IN from the layer during the passage of the wave. The visibility range of clouds formed and their scavenging effects over the range of possible IN number densities are shown schematically in Figure 2.

The solar, infrared, and net radiative forcings at the times of peak cloud optical depth are plotted versus IN number density in Figure 3. We define the radiative forcing as the change in net flux at the top of the atmosphere due to both the cloud and relative humidity increase At very low IN number densities, the radiative forcing is dominated by the relative humidity change; so the solar forcing is near zero, and the infrared forcing is positive Since these clouds are optically thin with relatively few large ice crystals, the infrared cloud radiative forcing dominates the solar forcing; hence, the net radiative forcing is positive, corresponding to a warming of the troposphere. The magnitude of the net radiative forcing increases with the IN number density. For IN number densities greater than 0 1 cm^{-3}, the net forcing exceeds 25 W m^{-2}.

The optical depth and radiative forcing of the cloud formed scales roughly linearly with the the assumed thickness of the supersaturated layer Hence, for narrower supersaturated layers, larger IN number densi-

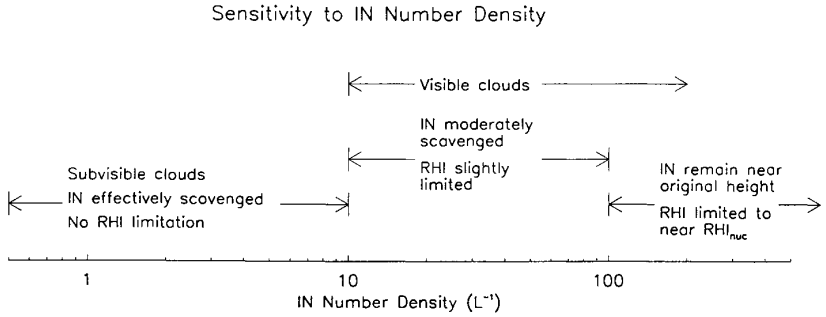

Figure 2. Schematic diagram of the sensitivity of clouds formed in moderately supersaturated regions to the IN number density. For $N_{IN} \leq 5$ x 10^{-3} to 2 x 10^{-2} cm^{-3} (depending on how large the ice crystals get), the clouds formed will be subvisible, the IN will be effectively removed from the supersaturated layer, and the ice crystal number densities will be too low to prevent unlimited humidity increase in updrafts. For larger N_{IN}, the clouds will be visible from the ground For $N_{IN} \geq 0.05$–0.1 cm^{-3}, the IN will not be substantially displaced vertically, and the RHI will be limited to near the threshold for ice nucleation.

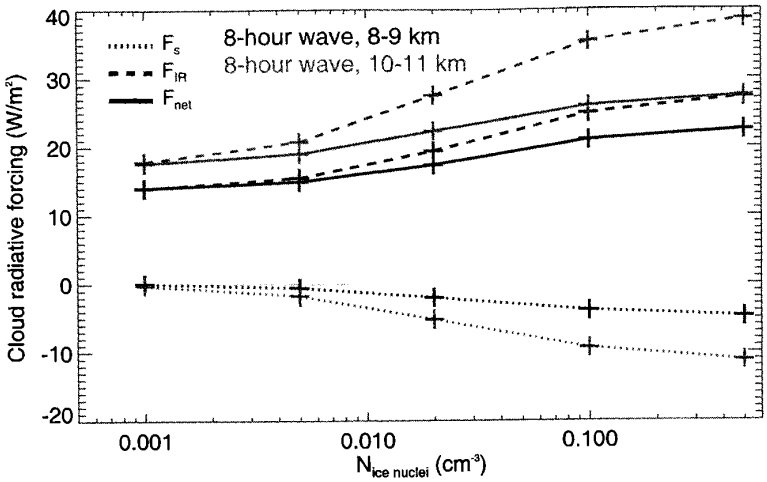

Figure 3. Solar, infrared, and net radiative forcing plotted versus IN number density for simulations with two different layer heights.

ties would be required to generate a visible cloud. Airborne lidar measurements of water vapor have shown that high water vapor mixing ratios in the upper troposphere often exist in narrow layers (a few hundred meters thick) [*Newell et al.*, 1996].

When the cloud forms at 8–8 5 km (-43° to -40°C) rather than 10-10.5 km (-59° to -56°C) the ice water content and cloud optical depth are larger due to the temperature dependence of ice saturation vapor pressure. Also due to the larger amount of water available, the ice crystals grow larger in the warmer clouds, and IN are scavenged more effectively. The period of the wave forcing the supersaturation has very little impact on the cloud optical depths, but it is important for the IN scavenging.

5. Discussion

The simulations described above suggest that if effective IN are present in the upper troposphere, then optically thin cirrus may form in supersaturated layers that never reach humidities high enough for freezing of sulfate haze aerosols. These clouds would generally not be detected by existing aircraft ice crystal sampling instrumentation. The optical depth and radiative forcing of these clouds is strongly sensitive to the number density of effective ice nuclei present.

Analysis of accurate in situ humidity measurements from recent aircraft missions indicates that ice supersaturation is very common in the upper troposphere. Even during time periods when no ice crystals were detected by the aircraft instrumentation, the air was ice supersaturated about 5–20% of the time. The fraction of horizontal area with supersaturation somewhere in the upper troposphere would necessarily be higher than the spatial fraction measured by in situ measurements, since supersaturation often occurs in thin layers. Hence, the fraction of the sky that could be covered by low optical depth ice clouds formed in moderately supersaturated regions is potentially very large. This fractional coverage would depend on the supersaturation frequency distribution and the IN activation spectrum (number of IN active versus supersaturation). The potential climatic impact of optically thin cirrus has been pointed out before [*Sassen et al.*, 1989]. The important result of this study is that the optical depth and radiative forcing of these cirrus may be extremely sensitive to the number density of ice nuclei present.

The sources, composition, and abundance of upper tropospheric IN are not well known Potential candidates include crustal mineral particles and soot particles from either aircraft exhaust or combustion at the surface [*Twohy and Gandrud*, 1998; *DeMott et al*, 1997; *Ström and Ohlsson*, 1998; *Petzold et al*, 1998]. If aircraft exhaust soot particles dominate IN number densities, then the optical depth and radiative forcing of cirrus in supersaturated regions should have been increasing rapidly over the past few decades and should continue to increase with increasing air traffic. If mineral dust particles are the dominant IN, then these optically thin cirrus should be annually variable following the strong seasonal variation in upper tropospheric dust loading [*Kent et al.*, 1995]. The midlatitude dust loading has a strong maximum in the spring.

This study suggests the plausibility of optically thin ice cloud formation in supersaturated regions of the upper troposphere. Improved measurements are required before a quantitative assessment of the global impact of these clouds will be possible. As was discussed ab11e, we currently only have a limited data set of in situ upper tropospheric humidity measurements. Additional in situ measurements and high spatial resolution re-

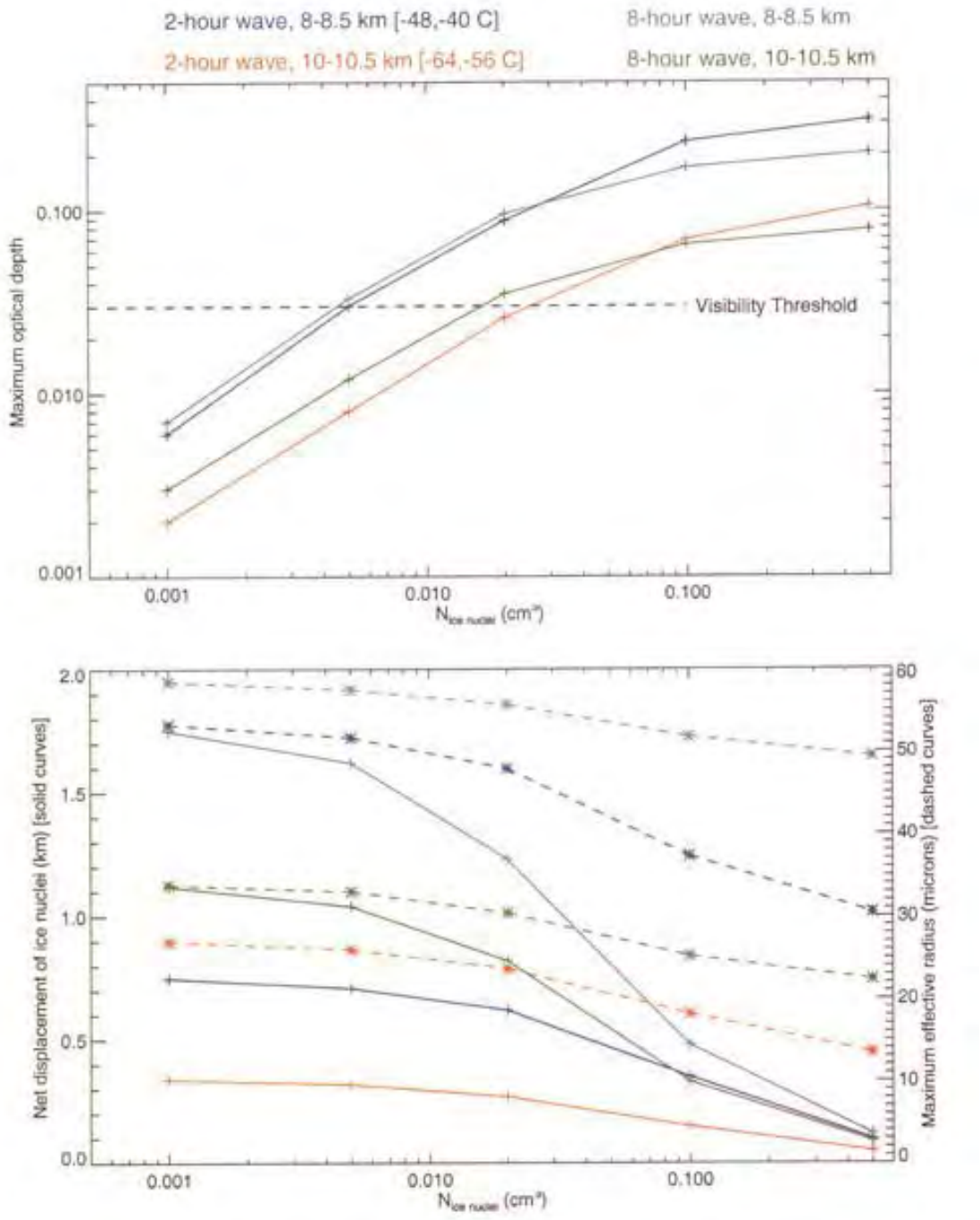

Plate 5. (top) Peak cloud optical depth plotted versus the initial IN number density (bottom) Effective vertical displacement of ice nuclei by cloud scavenging (solid curves) and maximum ice crystal effective radius (dashed curves) versus IN number density. The different curves correspond to simulations with the high humidity layer at different heights and different timescales for the imposed vertical motion.

12

mote sensing measurements would improve estimates of the fraction of the upper troposphere supersaturated with respect to ice For IN number densities larger than about 10^{-2} cm^{-3}, the clouds formed should have optical depths of the order of 0 01 or larger; so they should be easily detected by lidar [*Sassen et al.*, 1989]. *Goldfarb et al.* [2001] recently reported lidar measurements from a station in France indicating subvisible cirrus frequencies of about 18–25Space borne lidar or ground-based lidars at several locations could provide climatological information about optically thin cirrus. Also, direct measurements of the IN activation spectra at various locations in the upper troposphere are needed.

Acknowledgments. This research was supported by NASA's Upper Atmospheric Research Satellite Interdisciplinary Research Program, directed by Charles Jackman, and NASA's Stratospheric Aerosol and Gas Experiment, directed by Jack Kaye Support was also provided by NASA grants NAG1-2021 and NAG2-1258 to the University of Colorado The POLINAT 2 project was funded by the European Commission under contract ENV4-CT95-043

References

Baumgardner, D , J E Dye, and B W Gandrud, Interpretation of measurements made by the Forward Scattering Spectrometer Probe (FSSP-300) during the Airborne Arctic Stratospheric Expedition, *J Geophys Res , 97*, 8035, 1992

Clough, S A , M J Iacono, and J -L Moncet, Line-by-line calculation of atmospheric fluxes and cooling rates: Application to water vapor, *J Geophys Res , 97*, 15,761, 1992

DeMott, P J , D C Rogers, and S M Kreidenweis, The susceptibility of ice formation in upper tropospheric clouds to insoluble aerosol components, *J Geophys Res , 102*, 19,575, 1997

Gierens, K , U Schumann, M Helten, H Smit, and A Marenco, A distribution law for relative humidity in the upper troposphere and lower stratosphere derived from three years of MOZAIC measurements, *Ann Geophys , 17*, 1218, 1999

Goldfarb, L , P Keckhut, M -L Chanin, and A Hauchecorne, Cirrus climatological results from lidar measurements at OHP (44°N, 6°E), *Geophys Res Lett , 28*, 1687, 2001

Heymsfield, A J , L M Miloshevich, C Twohy, G Sachse, and S Oltmans, Upper tropospheric relative humidity observations and implications for cirrus ice nucleation, *Geophys Res Lett , 25*, 1343, 1998

Hintsa, E J , E M Weinstock, J G Anderson, R D May, and D F Hurst, On the accuracy of in situ water vapor measurements in the troposphere and lower stratosphere with the Harvard Lyman-α hygrometer, *J Geophys Res , 104*, 8183, 1999

Jensen, E J , and O B Toon, Ice nucleation in upper troposphere: Sensitivity to aerosol number density, temperature, and cooling rate, *Geophys Res Lett , 21*, 2019, 1994

Jensen, E J , et al , Ice nucleation in upper troposphere wave-clouds observed during SUCCESS, *Geophys Res Lett , 25*, 1363, 1998

Kelly, K K , A F Tuck, and T Davies, Wintertime asymmetry of upper tropospheric water vapor between the Northern and Southern Hemispheres, *Nature, 353*, 244, 1991

Kent, G S , P -H Wang, M P McCormick, and K M Skeens, Multiyear SAGE II measurements of upper tropospheric aerosol characteristics, *J Geophys Res , 100*, 13,875, 1995

Khvorostyanov, V I , and K Sassen, Cirrus cloud simulation using explicit microphysics and radiation, part II, Microphysics, vapor, and ice mass budgets, and optical and radiative properties, *J Atmos Sci., 55*, 1822, 1998

Koop, T , H P Ng, L T Molina, and M J Molina, A new optical technique to study aerosol phase transitions: The nucleation of ice from H_2SO_4 aerosols, *J Phys Chem , 102*, 8924, 1998

Miloshevich, L M , and A J Heymsfield, Under-measurement of high relative humidities in the upper troposphere by Väisälä RS80-A radiosondes, paper presented at the 10th Symp. on Meteorol Obs and Instrum , AMS, Phoenix, Ariz , Jan 11-16, 1998

Ovarlez, J , P van Velthoven, G Sachse, S Vay, H Schlager, and H Ovarlez, Comparison of water vapor measurements from POLINAT 2 with ECMWF analyses in high-humidity conditions, *J. Geophys Res , 105*, 3737, 2000

Newell, R E , and S Gould-Stewart, A stratospheric fountain?, *J Atmos Sci , 38*, 2789, 1981

Newell, R E , et al , Upper tropospheric water vapor and cirrus: Comparison of DC-8 observations, preliminary UARS microwave limb sounder measurements and meteorological analyses, *J Geophys Res , 101*, 1943, 1996

Petzold, A , J Ström, S Ohlsson, and F P Schröder, Elemental composition and morphology of ice-crystal residual particles in cirrus clouds and contrails, *Atmos Res , 49*, 21, 1998

Pruppacher, H R and J D Klett, *Microphysics of Clouds and Precipitation*, Kluwer Acad Norwell, Mass , 1997

Quante, M , P R A Brown, R Baumann, B Guillemet, and P Hignett, Three-aircraft intercomparison of dynamical and thermodynamical measurements during Pre-EUCREX campaign, *Beitr Phys Atmos , 69*, 129, 1996

Rogers, D C , P J DeMott, S M Kreidenweis, and Y Chen, Measurements of ice nucleating aerosols during SUCCESS, *Geophys Res Lett , 25*, 1383, 1998

Sassen, K , M K Griffin, and G C Dodd, Optical scattering and microphysical properties of subvisible cirrus clouds, and climatic implications, *J Atmos Sci , 28*, 91, 1989

Schumann, U , H Schlager, F Arnold, J Ovarlez, H Kelder, O Hov, G Hayman, I S A Isaksen, J Staehelin, and P D Whitefield, Pollution from aircraft emissions in the North Atlantic flight corridor: Overview on the POLINAT projects, *J Geophys Res , 105*, 3605, 2000

Ström, J , and S Ohlsson, In situ measurements of enhanced crystal number densities in cirrus clouds caused by aircraft exhaust, *J Geophys Res , 103*, 11,355, 1998

Tabazadeh, A , S T Martin, and J -S Lin, The effect of particle size and nitric acid uptake on the homogeneous freezing of aqueous sulfuric acid particles, *Geophys Res Lett , 27*, 1111–1115, 2000

Toon, O B , C P McKay, T P Ackerman, and K Santhaman, Rapid calculation of radiative heating and photodissociation rates in inhomogeneous multiple scattering atmospheres, *J Geophys Res., 94*, 16,287, 1989

Twohy, C H , and B Gandrud, Electron microscope analysis of residual particles from aircraft contrails, *Geophys Res Lett , 25*, 1359, 1998

Twohy, C H A J Schanot, and W A Cooper, Measurement of condensed water content in liquid and ice cl13ds using an airborne counterflow virtual impactor *J Atmos Oceanic Technol., 14*, 197, 1997

Udelhoffen, P M , and D L Hartmann, Influence of trop-

ical cloud systems on the relative humidity in the upper troposphere, *J. Geophys. Res., 100*, 7423, 1995

Vay, S , et al , Dc-8-based observations of aircraft CO, CH_4, N_2O, and $H_2O_{(g)}$ emission indices during SUCCESS, *Geophys. Res Lett., 25*, 1717, 1998

Vay, S A , B E. Anderson, E J Jensen, G W Sachse, J Ovarlez, G L Gregory, S R Nolf, J R Podolske, T A Slate, and C E Sorenson, Tropospheric water vapor measurements over the North Atlantic during the Subsonic Assessment Ozone and Nitrogen Oxide Experiment (SONEX), *J Geophys Res., 105*, 3745, 2000

Wang, P -H , P Minnis, M P McCormick, G S Kent, and K M Skeens, A 6-year climatology of cloud occurrence frequency from Stratospheric Aerosol and Gas Experiment II observations (1985–1990), *J. Geophys Res., 101*, 29,407, 1996

Warren, G , Optical constants of ice from the ultraviolet to the microwave, *Appl. Opt., 23*, 1206, 1984

T P Bui, E J Jensen, and R F Pueschel NASA Ames Research Center, MS 245-4, Moffett Field, CA 94035 (ejensen@sky arc nasa gov)

O B Toon, University of Colorado, LASP, Campus Box 392, Boulder, CO, 80309 (toon@lasp colorado edu)

S A Vay, NASA Langley Research Center, MS 483, Hampton, VA, 23681-2199 (s a vay@larc nasa gov)

J Ovarlez, Laboratoire de Meterologie Dynamique, Ecole Polytechnique, 91128 Palaiseau cedex, France (joelle ovarlez@polytechnique fr)

R May, SpectraSensors, Inc , 2400 Lincoln Avenue, Altadena, CA 91001 (rmay@spectrasensors com)

C H Twohy, Oregon State University, Oceanography Admin 104, Corvallis, OR 97331-5503 (twohy@OCE ORST EDU)

B W Gandrud, National Center for Atmospheric Research, ATD, Boulder, CO 80307 (gandrud@ucar edu)

U Schumann, Deutsches Zentrum fur Luft und Raumfahrt DLR-Institut fuer Physik der Atmosphaere, Oberpfaffenhofen, D-82230 Wessling, Germany (ulrich schumann@dlr de)

(Received October 14, 1999; revised July 17, 2000; accepted July 25, 2000)